

## Theoretical Study of Steam Condensation Induced Water Hammer Phenomena in Horizontal Pipelines

Imre Ferenc Barna, György Ézsöl and Attila Rikárd Imre

Department of Thermo Hydraulic Laboratory, Energy Research Center of the Hungarian Academy of Sciences, Hungary  
1121 Budapest, Konkoly Thege ut 29-33  
Telefon: +36-1-392-2222/1472  
Fax: +36-1-395-9293  
e-mail: barna.imre@energia.mta.hu

**Keywords:** steam condensation induced water hammer, WAHA3 model

### Abstract

We investigate steam condensation induced water hammer (CIWH) phenomena and present new theoretical results. We use the WAHA3 model based on two-phase flow six first-order partial differential equations that present one dimensional, surface averaged mass, momentum and energy balances. A second order accurate high-resolution shock-capturing numerical scheme was applied with different kind of limiters in the numerical calculations. The applied two-fluid model shows some similarities to Relap5 which is widely used in the nuclear industry to simulate nuclear power plant accidents. This model was validated with different CIWH experiments which were performed in the PMK-2 facility, which is a full-pressure thermo hydraulic model of the nuclear power plant of VVER-440/312 type in the Energy Research Center of the Hungarian Academy of Sciences in Budapest and in the Rosa facility in Japan. In our recent study we show the first part of a planned large database which will give us the upper and lower flooding mass flow rates for various pipe geometries where CIWH can happen. Such a reliable database would be a great help for future reactor constructions and scheming.

### Introduction

Safety of nuclear reactors is a fundamental issue. Nuclear and thermo-hydraulic processes in the active zone of modern reactors are well known and well-controlled, explosions are out of question. However, violent unwanted thermo-hydraulic transients in the primer loop may cause serious deformation or pipe breakage. Such an unplanned transient is the CIWM. In thermal loops of atomic reactors or in other pipelines where water steam and cold water can mix, quick and dangerous transients can happen causing pressure surges which mean high financial expenses or even cost human lives.

In the following we will present the WAHA3 model (I. Tiselj 2004), which is a complex physical model suitable to simulate various quick transients in single and two-phase flows, such as ideal gas Riemann problem, critical flow of ideal gas in convergent-divergent nozzle, rapid depressurization of hot liquid from horizontal pipes and column separation water hammer or even CIWH.

In the last two decades the nuclear industry developed a few complex two-phase flow-codes like Relap5 (Carlson 2003), Trac (Trac 1986) or Cathare (Bestion 2002) which are feasible to solve safety analysis of nuclear reactors and model complicated two-phase flow transients.

The model, WAHA3 has some similarities with Relap5. This means that the conservation equations are the same but the applied correlations are partially different.

The main difference between the above mentioned models and our WAHA3 code is basically the applied numerical scheme; other commercial codes have a ratio of spatial and time resolution  $\Delta x / \Delta t$  which describes usual flow velocities. WAHA3, however is capable of capturing shock waves and describe pressure waves which may propagate quicker than the local speed of sound. As a second point WAHA3 has a quick condensation model which is not available for Relap5 and Cathare.

### Nomenclature

|              |   |
|--------------|---|
| A            | pipe cross section ( $m^2$ )                            |
| $C_i$        | internal friction coefficient ( $kg/m^4$ )              |
| CVM          | virtual mass term ( $N/m^3$ )                           |
| $e_i$        | specific total energy [ $e = u + v^2/2$ ] (J/kg)        |
| $F_{g,wall}$ | wall friction per unit volume ( $N/m^3$ )               |
| g            | gravitational acceleration ( $m/s^2$ )                  |
| $h_i$        | specific enthalpy [ $h = u + p/\rho$ ] (J/kg)           |
| P            | Pressure (Pa)   |
| $p_i$        | interfacial pressure $p_i = p\alpha(1-\alpha)$ (Pa)     |
| $Q_{ij}$     | interf.-liq./gas heat transf. per vol. rate ( $W/m^3$ ) |
| t            | time (s)  |
| $u_i$        | specific internal energy (J/kg)                         |

|       |   |
|-------|---|
| $v_i$ | velocity (m/s)                                |
| $v_r$ | relative velocity ( $v_r = v_g - v_f$ ) (m/s) |
| $w$   | pipe velocity in flow direction (m/s)         |
| $x$   | spatial coordinate (m)                        |

**Greek letters**

|             |   |
|-------------|---|
| $\alpha$    | Vapour void fraction                      |
| $\Gamma_g$  | vapor generation rate ( $\text{kg/m}^3$ ) |
| $\rho_i$    | density ( $\text{kg/m}^3$ )               |
| $\vartheta$ | pipe inclination (degree)                 |

**Subscripts**

|   |              |
|---|--------------|
| l | Liquid phase |
| g | Gas phaset   |

$$\frac{\partial A(1-\alpha)\rho_l e_l}{\partial t} + \frac{\partial A(1-\alpha)\rho_l e_l (v_l - w)}{\partial x} + p \frac{\partial A(1-\alpha)}{\partial t} + \frac{\partial A(1-\alpha)p(v_l - w)}{\partial x} = A Q_{ij} - A \Gamma_g (h_l + v_l^2/2) + A(1-\alpha)\rho_l v_l g \cos\vartheta$$

(5)

$$\frac{\partial A\alpha\rho_g e_g}{\partial t} + \frac{\partial A\alpha\rho_g e_g (v_g - w)}{\partial x} + p \frac{\partial A\alpha}{\partial t} + \frac{\partial A\alpha p (v_g - w)}{\partial x} = A Q_{ij} + A \Gamma_g (h_g + v_g^2/2) + A\alpha\rho_g v_g g \cos\vartheta$$

(6)

**Experimental Facility**

This is a theoretical and numerical study, the used experimental facilities PMK2, and ROSA were mentioned in our former studies (Barna 2008, 2009, 2010, 2011).

**Numerical Scheme**

There are large number of different two-phase flow models with different levels of complexity(Stewart 1984, Menikoff 1989) which are all based on gas dynamics and shock-wave theory. In the following we present the one dimensional six-equation equal-pressure two-fluid model. The density, momentum and energy balance equations for both phases are the following:

$$\frac{\partial A(1-\alpha)\rho_l}{\partial t} + \frac{\partial A(1-\alpha)\rho_l (v_l - w)}{\partial x} = -A\Gamma_g \quad (1)$$

$$\frac{\partial A\alpha\rho_g}{\partial t} + \frac{\partial A\alpha\rho_g (v_g - w)}{\partial x} = A\Gamma_g \quad (2)$$

$$\frac{\partial A(1-\alpha)\rho_l v_l}{\partial t} + \frac{\partial A(1-\alpha)\rho_l v_l (v_l - w)}{\partial x} + A(1-\alpha) \frac{\partial p}{\partial x} - A \cdot CVM - A p_i \frac{\partial \alpha}{\partial x} = A C_i |v_r| v_r - A \Gamma_g v_l +$$

$$A(1-\alpha)\rho_l \cos\vartheta - A F_{l,wall} \quad (3)$$

$$\frac{\partial A\alpha\rho_g v_g}{\partial t} + \frac{\partial A\alpha\rho_g v_g (v_g - w)}{\partial x} + A\alpha \frac{\partial p}{\partial x} + A \cdot CVM + A p_i \frac{\partial \alpha}{\partial x} = -A C_i |v_r| v_r + A \Gamma_g v_g +$$

$$A\alpha\rho_g \cos\vartheta - A F_{g,wall} \quad (4)$$

Index l refers to the liquid phase and index g to the gas phase. Nomenclature and variables are described at the end of the manuscript. Left hand side of the equations contains the terms with temporal and spatial derivatives.

Hyperbolicity of the equation system is ensured with the virtual mass term CVM and with the interfacial term (terms with  $p_i$ ). Terms on the right hand side are terms describing the inter-phase heat, mass (terms with  $\Gamma_g$  vapor generation rate) volumetric heat fluxes  $Q_{ij}$ , momentum transfer (terms with  $C_i$ ), wall friction  $F_{g,wall}$ , and gravity terms. Modeling of the inter-phase heat, mass and momentum exchange in two-phase models relies on correlations which are usually flow-regime dependent.

The system code RELAP5 has a very sophisticated flow regime map with a high level of complexity. WAHA3 however has the most simple flow map with dispersed and horizontally stratified regimes only. The uncertainties of steady-state correlations in fast transients are very high.

A detailed analysis of the source terms can be found elsewhere (Tiselj 1997).

Two additional equation of states(eos) are needed to close the system of Eqs. (1-6). Here the subscript k can have two values 'l' for liquid phase, and 'g' for gas phase

$$\rho_k = \left( \frac{\partial \rho_k}{\partial p} \right)_k dp + \left( \frac{\partial \rho_k}{\partial u_k} \right)_p du_k.$$

(7)

Partial derivatives in Eq. 7 are expressed using pressure and specific internal energy as an input. The table of water and steam properties was calculated with a software from UCL (Seynhaeve 1984).

The system of Eqs. (1-6) represents the conservation laws and can be formulated in the following vectorial form

$$\underline{A} \frac{\partial \underline{\Psi}}{\partial t} + \underline{B} \frac{\partial \underline{\Psi}}{\partial x} = \underline{S}$$

(8)

where  $\bar{\Psi}$  represents a vector of the non-conservative variables  $\bar{\Psi}(p, \alpha, v_l, v_g, u_l, u_g)$  and  $\underline{A}, \underline{B}$  are 6-times-6 matrices and  $\bar{S}$  is the source vector of non-differential terms. These three terms can be obtained from Eq. (1-6) with some algebraic manipulation.

In this case the system eigenvalues which represent wave propagation velocities are given by the determinant  $\det(\underline{A} - \lambda \underline{B})$ . An improved characteristic upwind discretization method is used to solve the hyperbolic equation system (Eq. 8). The problem is solved with the combination of the first- and second-order accurate discretization scheme by the so-called flux limiters to avoid numerical dissipation and unwanted oscillations which appear in the vicinity of the non-smooth solutions. Exhaustive details about the numerical scheme can be found in the work of (LeVeque 1992).

## Results and Discussion

In our recent study we investigated pipe lines with three different diameters ( $D=10, 20, 50$  cm) with three different tube aspect ratio ( $L/D=25, 50, 75$ ) and with three different pressures ( $p=10, 20, 40$  bar).

These are physically relevant geometries with pressures values which are interesting in various nuclear facilities.

Table I presents these system parameters with the minimal and the maximal mass flow rates in between CIWH events happen.

For a better transparency these results are presented on Fig 1, 2 and 3 for the different pipe diameters. With this useful representation we can immediately see the dangerous CIWH range between the upper and lower flooding mass flow rates (see arrow in Fig 1.).

For completeness we explain additional technical details of our investigations. In all calculations we used the same nodalization in the sense that the actual length of the node is equal to the actual pipe diameter. In all calculations the same Courant-Friedrich-Levy limit was applied with 0.8. As numerical scheme the MINMOD limiter was used. There are only two exceptions at  $D=50, L/D=50, 75$   $p=20$  bar.

The temperature of the cold water was fixed to 293 K.

Each presented system (e.g.  $D=10$  cm,  $L/D=25$ ,  $p=20$  bar minimal mass flow rate) means at least 10 independent calculations with slightly different mass flow parameters.

For the maximal flow a calculation takes 20 minutes or even less but for the minimal flow rate one calculation might take 20 hours. To determine if a CIWH event happened we simple checked the pressure-time history closed to the cold water inlet visually. If a sharp peak with a 2 milisecond FWHM can be seen than we are in the dangerous water hammer region. It is worth to note that, our experience shows that there is a very sharp border at both sides of the CIWH regime in this WAHA3 model.

Unfortunately, the curves in Figure 1, 2, 3 are not parallel and cross each other which is a confusing problem at this moment. As explanation we think to say that, with additional very time consuming tuning of all the technical parameters (limiter, CFL condition, nodalisation) some of

the border points could be slightly modified, but this was not possible till now.

| System parameters | Minimal mass flow rate (kg/s) | Maximal mass flow rate (kg/s) |
|-------------------|-------------------------------|-------------------------------|
| <b>D = 10 cm</b>  |                               |                               |
| <i>L/D = 25</i>   |                               |                               |
| p = 10 bar        | 0.12                          | 7.64                          |
| p = 20 bar        | 0.12                          | 4.60                          |
| p = 40 bar        | 0.195                         | 4.60                          |
| <i>L/D = 50</i>   |                               |                               |
| p = 10 bar        | 0.23                          | 7.64                          |
| p = 20 bar        | 0.19                          | 5.46                          |
| p = 40 bar        | 0.23                          | 4.52                          |
| <i>L/D = 75</i>   |                               |                               |
| p = 10 bar        | 0.39                          | 3.9                           |
| p = 20 bar        | 0.27                          | 4.21                          |
| p = 40 bar        | 0.23                          | 4.29                          |
| <b>D = 20 cm</b>  |                               |                               |
| <i>L/D = 25</i>   |                               |                               |
| p = 10 bar        | 1.25                          | 42.08                         |
| p = 20 bar        | 1.25                          | 25.12                         |
| p = 40 bar        | 1.25                          | 27.75                         |
| <i>L/D = 50</i>   |                               |                               |
| p = 10 bar        | 1.187                         | 28.89                         |
| p = 20 bar        | 1.41                          | 25.43                         |
| p = 40 bar        | 1.41                          | 25.75                         |
| <i>L/D = 75</i>   |                               |                               |
| p = 10 bar        | 1.26                          | 26.38                         |
| p = 20 bar        | 1.26                          | 25.12                         |
| p = 40 bar        | 1.41                          | 26.70                         |
| <b>D = 50 cm</b>  |                               |                               |
| <i>L/D = 25</i>   |                               |                               |
| p = 10 bar        | 9.8                           | 266.5                         |
| p = 20 bar        | 9.8                           | 156.8                         |
| p = 40 bar        | 9.8                           | 160.0                         |
| <i>L/D = 50</i>   |                               |                               |
| p = 10 bar        | 9.8                           | 266.55                        |
| p = 20 bar        | 7.8                           | 519.4                         |
| p = 40 bar        | 13.7                          | 509.0                         |
| <i>L/D = 75</i>   |                               |                               |
| p = 10 bar        | 9.8                           | 262.66                        |
| p = 20 bar        | 9.8                           | 490.0                         |
| p = 40 bar        | 9.8                           | 505.6                         |

Table I the minimal and the maximal mass flow rates for the investigated systems.

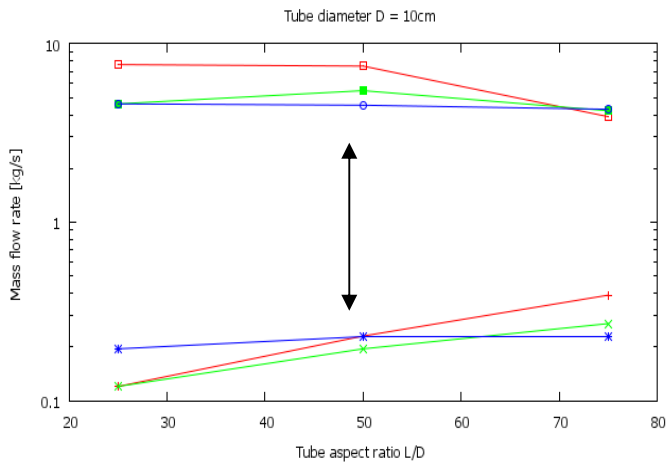


Figure .1. The minimal and maximal mass flow rates for the D=10 cm diameter pipelines for  $L/D = 25, 50, 75$  tube aspect ratios . Red curve is for  $p = 10$  bar, green curve is for  $p = 20$  bar, and the blue one is for  $p = 40$  bar.

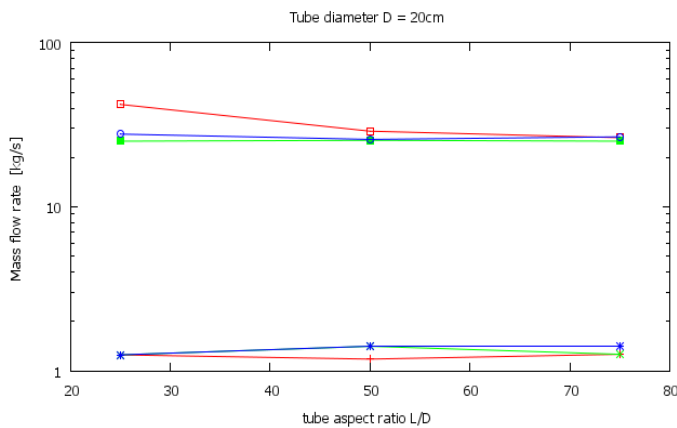


Figure .2. The minimal and maximal mass flow rates for the D=20 cm diameter pipelines for  $L/D = 25, 50, 75$  tube aspect ratios . Red curve is for  $p = 10$  bar, green curve is for  $p = 20$  bar, and the blue one is for  $p = 40$  bar.

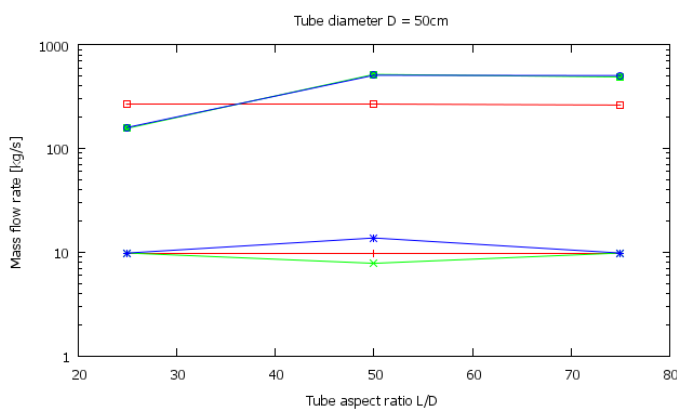


Figure .3. The minimal and maximal mass flow rates for the D=50 cm diameter pipelines for  $L/D = 25, 50, 75$  tube aspect ratios . Red curve is for  $p = 10$  bar, green curve is for  $p = 20$  bar, and the blue one is for  $p = 40$  bar.

## Conclusions

We presented the WAHA3 numerical model which is capable to describe supersonic two-phase flow transients in pipe lines. After our former studies (Barna 2008, 2009, 2010) we presented now a database where the minimal and maximal mass flow rates can be determined for large number of flow systems. We plan to go further and enhance our database for even larger number of systems.

## Acknowledgements

We thank Prof. Dr. Iztok Tiselj (Jozef Stefan Institute, Ljubljana, Slovenia) for his fruitful discussions and valuable comments.

## References

- I. Tiselj, A. Horvath, G. Cerne, J. Gale, I. Parzer, B. Mavko, M. Giot, J.M. Seynhaeve, B. Kucienska and H. Lemonnier, WAHA3 code manual, Deliverable D10 of the WAHALoads project, March 2004
- K.E. Carlson, R.A. Riemke, S.Z. Rouhani, R. W. Shumway and W. L. Weaver RELAP5/MOD3.3Beta Code Manual, Vol 1-7, NUREG-CR/5535, EG&G Idaho, Idaho Falls 2003
- TRAC-PF1/MOD1: An Advanced Best-Estimate Computer Program for Pressurized Water Reactor Thermal-Hydraulic Analysis, NUREG/CR-3858, L.A-10157-MS, 1986
- D. Bestion and G. Geffraye, "The CATHARE code" CEA Grenoble Report, DTP/SMTH/LMDS/EM/22001-63, April 2002
- I. Tiselj and S. Petelin "Modeling of Two-Phase Flow with Second-Order Accurate Scheme" Journal of Comput. Phys. 136, 503- 521 (1997)
- M-H. Chun and S-O. Hu, "A parametric study and a guide to avoid condensation-induced water hammer in a horizontal pipe" Nucl. Eng. and Des. 201, 239 (2000)
- H.B. Stewart and B. Wendroff, "Two-Phase flow: Models and Methods" J. Comp. Phys. 56, 363 (1984)
- R. Menikoff. and B. Plohr, "The Riemann Problem fluid flow of real materials" Rev. Mod. Phys. 61, 75-130 (1989)
- J.M. Seynhaeve, Water properties package, Catholic University of Louvain (1992) Project Built with IAPS from Lester, Gallaher and Kell, McGraw-Hill 1984
- R. J. LeVeque Numerical Methods for Conservation Laws, Lecture in Mathematics, ETH, Zurich, (1992)

I. F. Barna, G. Baranyai and Gy Ezsol  
" 8095 Theoretical and Experimental Study of Steam  
Condensation Induced Water Hammer Phenomena "  
Proceedings of the 2008 International Congress on  
Advances in Nuclear Power Plants, Anaheim CA  
USA, June 8-12 2008

I. F. Barna, G. Baranyai and Gy Ezsol  
" 9003 Experimental and Theoretical Study of Steam  
Condensation Induced Water Hammer Phenomena "  
Proceedings of the 2009 International Congress on  
Advances in Nuclear Power Plants, Tokyo, May 10-14  
2009

I. F. Barna, L. Varga and Gy Ezsol  
" Steam Condensation Induced Water Simulations for  
Different Pipelines in Nuclear Reactor "  
Proceedings of the 8th International Topical Meeting  
of Nuclear Thermo-Hydraulics, Operation and Safety  
NUTOS-8 Shanghai, China October 10-14, 2010

I.F. Barna and Gy. Ezsol  
Steam Condensation Induced Water Hammer  
Simulations for Different Pipelines  
The 14th International Topical Meeting on Nuclear  
Reactor Thermalhydraulics, NURETH-14 Toronto,  
Ontario, Canada, September 25-30, 2011  
NURETH14-xxx

I.F. Barna, A.R. Imre, G. Baranyai and Gy. Ezsol,  
" Experimental and theoretical study of steam  
condensation induced water hammer phenomena"  
Nuclear Engineering and Design 240, (2010) 146